Colloid Polym Sci (2005) 284: 80–85
DOI 10.1007/s00396-005-1327-0

SHORT COMMUNICATION

C. Dushkin
K. Papazova
N. Dushkina
E. Adachi

Attenuated quantum confinement of the exciton in semiconductor nanoparticles

Received: 18 October 2004
Accepted: 14 January 2005
Published online: 15 July 2005

C. Dushkin (✉)
Group of Nanoparticle Science and Technology, Department of General and Inorganic Chemistry, Faculty of Chemistry, University of Sofia, 1, James Bourchier Blvd, 1126 Sofia, Bulgaria

K. Papazova
Group of Nanoparticle Science and Technology, Department of General and Inorganic Chemistry, Faculty of Chemistry, University of Sofia, 1 James Bourchier Blvd, 1126 Sofia, Bulgaria

N. Dushkina
Department of Physics, University of Millersville, Millersville PA 17551-0302, USA

E. Adachi
Nihon L'Oreal Research Center, 3-2-1 Sakado, Takatsu-ku, Kawasaki, Kanagawa 213-0012, Japan

Abstract A new effect, called attenuated quantum confinement, is described using a theoretical approach, based on the effective mass approximation. It assumes that the exciton, generated in a semiconductor nanocrystal, can penetrate the medium outside the crystal boundary. An equation is derived for the energy of attenuated quantum confinement depending on the penetration depth and mass of exciton outside the crystalline core. It gives lower absorption energy, which is observed experimentally for very small nanocrystals, compared to that predicted by usual quantum confinement. The penetration depth calculated for compound semiconductors is found to be of the same magnitude as that of the thickness of organic capping layer for CdS, CdSe, PbS and InAs nanoparticles. Our finding can also explain other practical processes of charge generation and transportation in a matrix with embedded nanocrystals.

Keywords Semiconductor nanoparticle · Attenuated quantum confinement · CdS · CdSe · PbS · InAs

Introduction

A semiconductor nanoparticle consists of a nanocrystal core (semiconductor) of radius R, capped with an organic layer of thickness δ covalently bound to crystalline surface during the synthesis process (see Fig. 1a). For semiconductor nanoparticles, the most striking observation is that the wavelength of emission depends on the nanocrystal size, see for example, the beautiful color produced by CdSe nanocrystals in Ref. [1]. In this case the nanoparticles, dispersed in organic liquid medium and excited with UV-light, can be considered as isolated emitters of light. The variation of photoluminescence and absorbance wavelength with the particle size is theoretically explained as a quantum confinement (QC) effect, considering the exciton fully confined in the physical dimensions of nanocrystal core [2–4]. The energy of the lowest 1s-excited state is then given by the following expression [4]:

$$E(R) = E_g + \frac{\pi^2\hbar^2}{2m_1R^2} - \frac{1.786e^2}{\varepsilon_1 R} - \frac{0.248m_1e^4}{2\varepsilon_1^2\hbar^2}, \quad (1)$$

Here, E_g is the energy band gap for bulk semiconductor, $\hbar = 1.055 \times 10^{-34}$ J · s is Planck constant, m_1 is effective

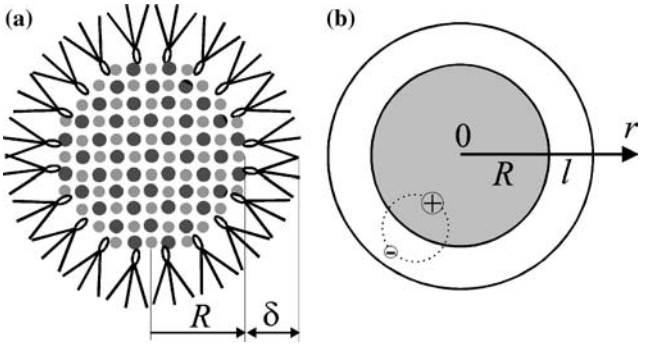

Fig. 1 **a** Semiconductor nanoparticle with a crystalline core of radius R and organic capping layer of thickness δ; **b** model of a nanoparticle with two domains for exciton motion: inner ($0 \le r \le R$) and outer ($R \le r \le R+l$)

mass of the exciton, $e = 1.602\times10^{-19}$ C is electron charge, $\varepsilon_1 = 4\pi\,\varepsilon_0\,\varepsilon_{1r}$ is dielectric constant of the material with $\varepsilon_0 = 8.854\times10^{-12}$ F/m being the permittivity of vacuum and ε_{1r} the relative dielectric constant. The second term on the right-hand side of Eq. 1 represents the quantum confinement energy $E_{QC} = \pi^2\hbar^2/2m_1R^2$, which dominates for particles of small radii R. The Coulomb energy, E_C, given by the third term, is of importance for relatively big particles. The Rydberg energy, E_R, given by the fourth term, is related to the electron–hole correlation. Although E_R is a rather small constant and could be omitted [4], we will preserve it for completeness.

Equation 1 fails to explain experimental data for the energy deduced from absorbance spectra of nanoparticle suspensions (CdS [5], PbS [6] and CdSe [7]) plotted versus the radius of nanocrystal core R. The core radius is usually measured by transmission electron microscope (TEM). The calculated energy is substantially larger for very small nanocrystals, which can lead to overestimated nanocrystal radius by up to 100% [6, 7] (cf. Figs. 4 and 5) This represents a significant problem for the synthesis [8] and manufacturing [9] of nanoparticles, where one has to control their size from the absorbance spectra recorded during the nanocrystal growth. Since Coulomb term E_C is not enough to count down the right functional dependence on R, one has to look for another solution whereby the contribution of the QC term, E_{QC}, is appreciably decreased. For example, assuming that nanoparticle radius in the denominator is effectively larger than that of nanocrystalline core. This effect of the exciton travelling outside the core, seen in Fig. 1b, is denoted by us as attenuated quantum confinement (AQC).

Experimental evidence for such a possibility is given by the phenomena of electron charge exchange between nanocrystals incorporated in a matrix. The possibility for an electron to delocalize outside nanocrystal core is confirmed for a single semiconductor nanoparticle (CdSe), leading to ionization/deionization process as shown by intermittent fluorescence light [10]. If nanocrystals such as CdSe or CdS are embedded in glass, the released electron can become trapped in host matrix, which in fact is used to explain the effect of persistent hole burning [11]. Another example is excitation-time dependent photoluminescence discovered in a thin film of CdSe nanoparticles exposed to UV-light [12]. The photoluminescence intensity increases upon excitation due to electrons release by nanocrystal cores; then the electrons accumulate in the organic matrix of capping agent, tri-octylphosphine oxide (TOPO), and can exchange among cores.

On the basis of these observations, one can make the following assumptions: (1) In the case of isolated nanoparticles on a substrate or in an isolating matrix, the electron can go outside the core and stay in the vicinity of nanocrystal surface. The shell of electron localization may not exceed the boundary of organic capping layer. (2) For nanoparticles in a conducting medium, the electrons from the shell can hop to more distinct domains. In both cases (1) and (2), this will violate the effect of QC by increasing the space for motion of the exciton until the electron and hole can be correlated in a couple.

The purpose of our paper is to outline a simple theory of attenuated quantum confinement based on effective mass approximation—the model used to calculate exciton energy. The result is an energy expression accounting for the degree of exciton penetration outside nanocrystal core, which is in a very good agreement with experimental data. This allows calculating the true nanocrystal radius from absorption energy by knowing one more parameter of the system—the exciton penetration depth l. The latter is obtained by fitting experimental data for compound semiconductors such as CdS, CdSe, PbS and InAs.

Theoretical model

In Fig. 1b, we consider the exciton (the couple of hole and electron) that is localized in both media with the hole staying preferably in the nanocrystalline core and the electron penetrating in a shell of thickness l ($l \sim\delta$). Schrödinger equations describing exciton motion are as follows:

$$\frac{\hbar^2}{2m_i}\Delta_r\psi_i + E_i\psi_i = 0, \qquad (2)$$

where $\Delta_r = r^{-2}(\mathrm{d}/\mathrm{d}r)r^2(\mathrm{d}/\mathrm{d}r)$. Subscript $i=1$ refers to the core ($0 \le r \le R$) and $i=2$ refers to the shell ($R \le r \le R+l$). The effective mass of exciton, m_i, is given by $1/m_i = 1/m_{ih} + 1/m_{ie}$, where m_{ih} is the mass of hole and m_{ie} is the mass of electron in the respective

medium i. In our calculations, we assume that $E_i = E$ in both the core and shell, where E is quantum energy of nanocrystal. First, this means that we neglect any small energy barrier, which may exist between the two media; as a result, any difference in the exciton motion comes only from the different effective masses of carriers. Second, the energies, E_i, should contain respective electrostatic energy terms, which are also omitted for the sake of the simplicity of calculations. The wave functions, ψ_i and their derivatives, have to match at the core boundary; subsequently $\psi_1(R) = \psi_2(R)$; $m_1^{-1}(\mathrm{d}\psi_1/\mathrm{d}r)|_R = m_2^{-1}(\mathrm{d}\psi_2/\mathrm{d}r)|_R$ (the latter comes from balance between the fluxes across the interface). The wave function should be finite at the core center, $\psi_1(0) = \text{const}$, and should vanish outside the nanoparticle, $\psi_2(R+l) = 0$.

The substitution, $\psi_i = \phi_i / r$, transforms Eq. 2 into the equation $\mathrm{d}^2\varphi_i/\mathrm{d}r^2 + k_i^2\varphi_i = 0$, where $k_i = \sqrt{2m_iE_i}/\hbar$ is the wave number. This equation is easily solved for the function, ϕ_i, thus giving for the wave functions,

$$\psi_i(r) = A_i \sin(k_i r)/k_i r + B_i \cos(k_i r)/k_i r. \tag{3}$$

From the conditions for ψ_i, the constants in Eq. 3 are found to obey the relationships $A_2 = A_1 k_2 \sin(k_1 R)\{k_1 \sin(k_2 R)[1 - \tan k_2(R+l)/\tan(k_2 R)]\}^{-1}$, $B_1 = 0$, $B_2 = -A_2 \tan k_2(R+l)$. Replacing them in the boundary condition for fluxes gives the following relationship for wave numbers:

$$\begin{aligned}(-1 + x\cot x)\left\{1 - \cot(x/\sqrt{\mu})\tan[(1+\beta)x/\sqrt{\mu}]\right\} \\ = \mu\left\{-1 + (x/\sqrt{\mu})\cot(x/\sqrt{\mu}) \right. \\ \left. + \left[x/\sqrt{\mu} + \cot(x/\sqrt{\mu})\right]\tan[(1+\beta)x/\sqrt{\mu}]\right\}.\end{aligned} \tag{4}$$

Here, $x = k_1 R$ and $\beta = l/R$; the parameter, $\mu = m_1/m_2$, is the ratio between effective masses of the exciton. In the simplest case of two uniform media $\mu = 1$, because $m_1 = m_2$. If we take $k_1 = k_2$, Eq. 4 simplifies to $\tan k_1(R+l) = 0$ with the solution $k_1 = n\pi/(R+l)$, where $n = 1,2,3,\ldots$. Thus, the leading term in AQC energy is obtained:

$$E_n^{(0)} = \frac{\pi^2\hbar^2 n^2}{2m_1(R+l)^2}. \tag{5}$$

Numerical solution of Eq. 4 gives the exact energy levels. Here, we look for analytical solution assuming a small difference of exciton masses, i.e., $\alpha = (m_2 - m_1)/m_2 = 1 - \mu$ is much smaller than unity. Expanding the arguments and trigonometric functions in series of α lead to the following expressions: $x^{(0)} = n\pi/(1+\beta)$ (cf. Eq. 5) and

$$\begin{aligned}x^{(0)}x^{(1)} = \frac{\cos^2 x^{(0)}}{(1+\beta)(1+\cot^2 x^{(0)})}\left\{1 - x^{(0)}\tan x^{(0)}\right. \\ + \frac{x^{(0)}}{2}\left[\cot x^{(0)} + \frac{(1+\beta)x^{(0)}}{\cos^2 x^{(0)}}(1+\cot^2 x^{(0)})\right. \\ \left.\left. - \frac{x^{(0)}}{\sin^2 x^{(0)}}\right]\right\}.\end{aligned}$$

Here $x = x^{(0)} - \alpha x^{(1)}$, $k = k^{(0)} - \alpha k^{(1)}$ and $E(\alpha) = E^{(0)} - \alpha E^{(1)}$. Respective energy terms are $E^{(0)} = \hbar^2 k_1^{(0)^2}/2m_1$ and $E^{(1)} = \hbar^2 k_1^{(0)} k_1^{(1)}/m_1$, where $R^2 k_1^{(0)} k_1^{(1)} = x^{(0)}x^{(1)}$. Subsequently, quantum energy of the nanocrystal is

$$E_{\mathrm{AQC}} = \frac{\pi^2\hbar^2}{2m_1(R+l)^2} - \alpha\frac{\hbar^2}{m_1R^2}x^{(0)}x^{(1)}. \tag{6}$$

The first term in the right-hand side of Eq. 6 differs from the respective term, E_{QC}, in Eq. 1 by quantity l in the denominator, which is the thickness of localization layer of exciton around the core. Therefore, l has the meaning of a penetration depth, which increases the space of exciton motion beyond the physical dimension of semiconductor core. Mathematically, it results in a smaller energy as compared to that corresponding to usual QC at $l = 0$. As shown below, this fact explains well the discrepancy between experiment and theory. The second term acts so as to increase the QC energy if $m_2 > m_1$, which turns out to be the usual case for nanoparticles that are considered here. This term is much smaller than the first term, but it accounts for the difference of exciton masses in the core and shell. In Eq. 1, replacing E_{QC} with E_{AQC} leads to a counterpart of Eq. 1 in the approximation of attenuated quantum confinement

$$\begin{aligned}E(R) = E_g + \frac{\pi^2\hbar^2}{2m_1(R+l)^2} - \alpha\frac{\hbar^2}{m_1R^2}x^{(0)}x^{(1)} - \frac{1.786e^2}{\varepsilon_1 R} \\ - \frac{0.248m_1e^4}{2\varepsilon_1^2\hbar^2}.\end{aligned} \tag{7}$$

Equation 7 will be used in fitting the experimental data throughout the paper. The typical magnitudes of different terms for CdS at $R = 10$ Å are the following: 1st term 2.3 eV, 2nd term 1.45 eV, 3rd term 0.18 eV, 4th term −0.48 eV, 5th term −0.018 eV.

Results and discussion

The wave function calculated by Eq. 3 is plotted in Fig. 2 for CdSe nanocrystal of radius $R = 14.9$ Å at the following values of other parameters: $l = 8.4$ Å, $\mu = 1.029$, $k_1 = 0.135$ Å^{-1}, $k_2 = 0.133$ Å^{-1}, $A_1 = 1$, $A_2 = 0.993$, $B_2 = 0.044$. For comparison, the wave function obtained by the usual QC is

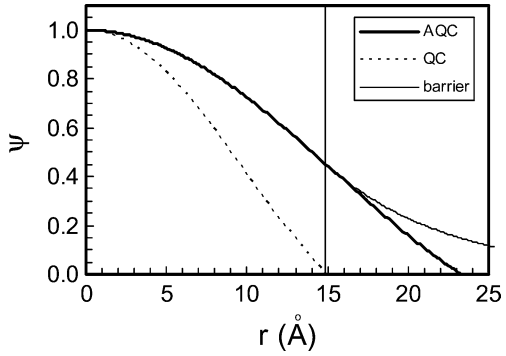

Fig. 2 Wave functions of the exciton calculated based on different assumptions: infinite potential barrier located on the core surface at $r = R$ (usual quantum confinement, QC), infinite potential barrier located at a distance $r = R + l$ (attenuated quantum confinement, AQC), and finite potential barrier on the core surface (barrier)

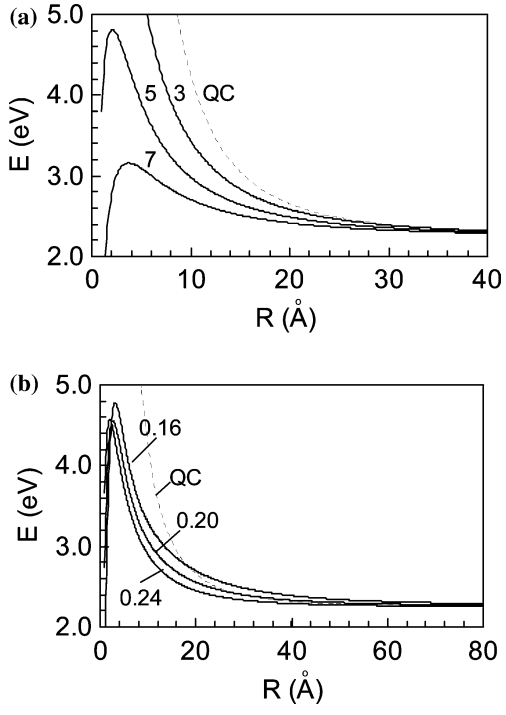

Fig. 3 Numerical simulations with Eq. 7 for nanoparticles of CdS: **a** constant $m_2/m_0 = 0.17$ ($\mu = 0.9031$) and different l plotted in Å ; **b** constant $l = 5.2$ Å and different ratio m_2/m_0 plotted on the curves

$$\psi_1 = A_1 \sin(k_1 r)/k_1 r. \tag{8}$$

Hence, k_1 is given as $k_1 = \pi/R = 0.211$ Å^{-1}. The pronounced difference between the two functions explains the delocalization of exciton farther than the vertical line at the position of nanocrystal radius. This leads to smaller energy of quantum confinement as calculated below. The portion of wave function situated outside nanocrystal core is smaller than the long tail obtained, assuming finite potential barrier, U_0, at nanocrystal

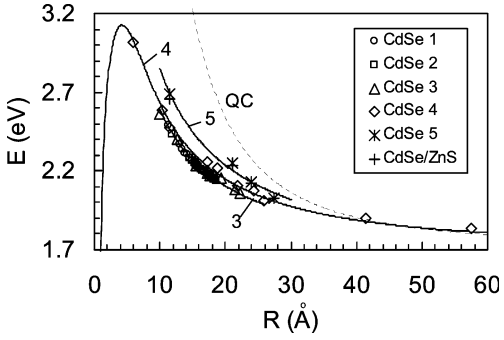

Fig. 4 Comparison of the predictions of Eq. 7 with experimental data for the energy derived from the absorption spectra of CdSe nanoparticles in solution. The fitting parameters are summarized in Table 1. The data points are taken from the literature, at different capping layers resulting from the synthesis method: TOPO + TBP (1, 2 [8] and 3 [8]); TOPO + TOP (4 [7] and 5 [1]); CdSe/ZnS core-shell particles [1]

surface. In this case, the respective equation for the shell is $\Delta_r \psi_2 - k_2^2 \psi_2 = 0$, where the energy is given as $E_2 = U_0 - E$. Matching the two wave functions, ψ_1, given by Eq. 8 and $\psi_2 = B_2 e^{-k_2 r}$, lead to the following expression for constant $B_2 = A_1 \sin(k_1 R) e^{-k_2 R}/k_1 R$. The energy can be calculated by using the expression $\tan x = x/\left[1 - \sqrt{\mu^2(x_0^2 - x^2)}\right]$, where $x_0 = k_0 R$ and $k_0 = \sqrt{2 m_1 U_0}/\hbar$. Numerical calculation at typical values, $U_0 \sim 0.5$ eV, gave always smaller quantum energy than experimental data, which implies that the model of small surface barrier underestimates the contribution of quantum confinement.

Figure 3 plots the energy from Eq. 7 at different values of the parameters for particular semiconductor nanoparticles of CdS. At a fixed effective mass, m_2 (Fig. 3a), increasing the penetration depth, l, decreases the energy of AQC far below the values of the usual QC. The curve passes through a maximum before which the third term in Eq. 7 becomes large and negative; hence, it compensates the second term and the total energy E decreases. Such behavior seems quite reasonable in view of the vanishing energy for very small nanoparticles compared to the infinite energy predicted by Eq. 1 at $R \to 0$. Similarly, for fixed depth l, increasing the effective mass, m_2, leads to a decrease of the energy (Fig. 3b). At large particle radii ($R \to \infty$), the energy for both models tends to the constant value, E_g, in accord with the asymptotes of Eqs. 1 and 7.

Our model for AQC is compared with the experimental data for the ground energy of exciton for various semiconductors in Figs. 4 and 5 and in Table 1. For CdSe, the agreement between our theory and the experiment is remarkable for the nanoparticles synthesized by various authors (see Fig. 4). At the same time, it allows distinguishing tiny variations of synthesis conditions that affect nanocrystal energy. For example, syn-

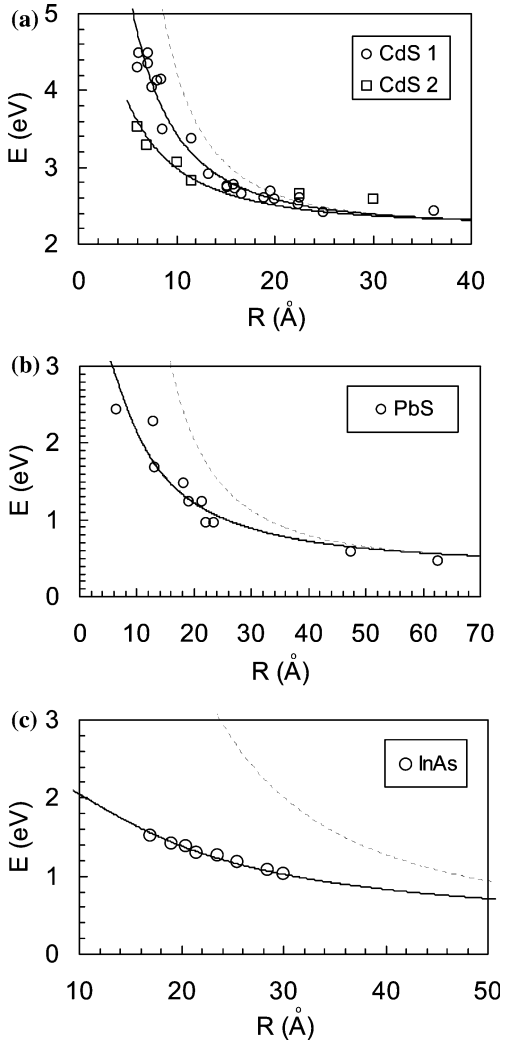

Fig. 5 Fit of experimental data for various nanoparticles: **a** CdS (1 [4, 12] and 2 [14]); **b** PbS [5, 14]; **c** InAs [15]

theses at the same conditions (CdSe1 and CdSe2 [9]) have nearly the same fitting parameters averaged in Table 1. Syntheses carried out in two different laboratories [8, 9], but using the same conditions, lead to nanoparticles with slightly different energetic properties and hence penetration depth was $l = 9.1$ and 8.2 Å, respectively. The capping layer in both cases is composed of tri-octylphosphine oxide (TOPO) coming from the matrix plus inclusions of tri-butylphosphine (TBP), the binding agent for selenium as a precursor [9]. Using another recipe of synthesis with tri-octylphosphine (TOP) in the precursor [7] leads to a pronounced difference in nanoparticles: at one and the same core radius, they exhibit higher absorbance energy by about 0.2 eV (blue shift of 12 nm). Assuming core material with the same properties, as confirmed by the respective fitting parameters, the observed difference can be attributed to the capping layer. The latter contains only octyphosphine compounds, which make it denser as seen from the higher effective mass m_2. The nanoparticles from Ref. [1] are of even higher energy attributed to larger m_2.

A shell of few atomic layers of ZnS does not appreciably affect the absorption energy as seen from the comparison with series CdSe/ZnS nanoparticles-from Ref. [1]. It means that this shell is almost equivalent to the organic capping layer with respect to exciton motion. At the same time, the capping of CdSe with wide-zone semiconductor, such as ZnS or CdS [17], was found very efficient with respect to high quantum yield and luminescence intensity. The dependence of photoluminescence as a function of the nanoparticle size is not a simple issue and goes beyond the scope of our paper.

Two series of CdS nanoparticles with pronounced difference in the energy versus R are shown in Fig. 5a. This leads to rather different values of penetration depth l in Table 1 for nearly the same effective masses, m_2, in the shells. Most probably, the two batches are of varying composition and/or structure due to the various ways of synthesis. The different band gaps, E_g, accepted for the series, 2.3 and 2.4 eV, both of them being smaller than the value for bulk CdS (2.58 eV), support the above.

For narrow band-gap semiconductors such as PbS (Fig. 5b) and InAs (Fig. 5c), the situation is rather similar to that described above. The biggest difference between calculated energy in AQC and QC approximations is observed for InAs where the penetration depth is noticeably larger.

Considering the full set of data in Table 1, one can conclude that, with some exceptions, penetration depth is almost constant, $l \sim 8$–10 Å, for most of the materials. This value is comparable with the thickness of organic capping layer. Therefore, the nanocrystal core and organic shell can be considered as two inseparable parts of one undivided object—the nanoparticle. The match between these two parts seems so precise that the exciton does not feel a difference while travelling in any of them. In support to this conclusion is the very small difference between the effective mass m_2 in the shell and m_1 in the core (see μ in Table 1).

Conclusion

A new effect is considered using the model of attenuated quantum confinement due to penetration of the exciton in the organic shell outside the crystalline core of a semiconductor nanoparticle. On the basis of this assumption, a new expression is derived for quantum confinement energy whose leading terms contain the penetration depth of the exciton outside the core and the effective mass of the exciton in the shell. This equation describes experimental data for energy with a good

Table 1 Model parameters for nanoparticles of compound semiconductor materials

Semiconductor core	Capping shell layer	E_g (eV)	ϵ_{1r}	m_e/m_0 [a]	m_h/m_0 [a]	m_1/m_0 [a]	m_2/m_0 [a]	μ	l (Å)
CdS	HMP [4, 13]	2.3[b]	5.4[f]	0.19[c]	0.8[c]	0.154	0.170	0.903	3.0
	TP [15]	2.4[b]					0.179	0.858	5.2
CdSe	TOPO + TBP [8]	1.74[d]	10.0[f]	0.13[f]	0.45[f]	0.101	0.117	0.862	9.1
	TOPO + TBP [9][g]						0.103[h]	0.975[h]	8.2[h]
	TOPO + TOP [7]						0.140	0.720	9.4
	TOPO + TOP [1]						0.144[i]	0.695[i]	8.0[i]
PbS	E-MAA [6, 15]	0.41[e,f]	17.0[f]	0.11[e]	0.11[e]	0.055	0.069	0.797	10.1
InAs	TOP [16]	0.36[d,f]	14.6[f]	0.026[d]	0.41[d]	0.0244	0.0300	0.815	19.1

[a] Taken relatively to the electron mass, $m_0 = 9.11 \times 10^{-31}$ kg
[b] Literature value, $E_g = 2.58$ eV [3, 14]
[c] Data from Ref. [3]
[d] Data from Ref. [14]
[e] Data from Ref. [6] (close value for E_g is also 0.37 eV [14])
[f] Data from Ref. [18]
[g] The data from Ref. [9] are calculated from the optical spectra. The rest of data are measured by TEM
[h] Average values from the two experiments: CdSe1 and CdSe2
[i] Average values from the two experiments: CdSe5 and CdSe/ZnS
List of organic components: *HMP* hexamethaphosphate; *TP* thiophenolate; *TOPO* tri-octylphosphine oxide; *TBP* tri-butylphosphine; *TOP* tri-octylphosphine; *E-MMA* ethylene-15% methacrylic acid copolymer

accuracy, which allows determining the true nanocrystal radius directly from the absorbance spectrum of a nanoparticle suspension.

The model parameters are calculated for a variety of semiconductor nanoparticles: CdS, CdSe, PbS and InAs. The penetration depth is found to be nearly the same magnitude for most materials, i.e., about 8–10 Å, roughly corresponding to the thickness of organic shell layer capping the nanocrystal core. The small difference in the corresponding effective masses of exciton in the two media refers to the formation of interfacial layer of smooth transition between the core and shell.

Our findings can be used to control nanocrystal growth by obtaining nanocrystal size from the absorbance of nanoparticle suspension measured *in situ*. Also, they can serve as a test for the degree of matching between the semiconductor material and the organic matrix, most probably depending on the synthesis conditions.

References

1. Dabbousi BO, Rodriguez-Viejo J, Mikulec FV, Heine JR, Mattoussi H, Ober R, Jensen KF, Bawendi MG (1997) J Phys Chem B 101:9463
2. Efros AlL, Efros AL (1982) Sov Phys Semicond 16:772
3. Brus LE (1983) J Chem Phys 79:5566
4. Yoffe AD (1993) Adv Phys 42:173
5. Weller H, Schmidt HM, Koch U, Fojtik A, Baral S, Henglein A, Kunath W, Weiss K, Dieman E (1986) Chem Phys Lett 124:557
6. Wang Y, Herron N, Mahler W, Suna A (1989) J Opt Soc Am B 6:808
7. Murray CB, Norris DJ, Bawendi MG (1993) J Am Chem Soc 115:8706
8. Peng X, Wickham J, Alivisatos AP (1998) J Am Chem Soc 120:5343
9. Dushkin CD, Saita S, Yoshie K, Yamaguchi Y (2000) Adv Colloid Interface Sci 88:37
10. Nirmal M, Dabbousi BO, Bawendi MG, Macklin JJ, Trautman JK, Harris TD, Brus LE (1996) Nature 383:802
11. Masumoto Y (1996) J Luminescence 70:386
12. Maenosono S, Dushkin CD, Saita S, Yamaguchi Y (2000) Japan J Appl Phys Part 1 39:4006
13. Fojtik A, Weller H, Koch U, Henglein A (1984) Ber Bunsenges Phys Chem 88:969
14. Kittel C (1986) Introduction to solid state physics. Wiley, New York
15. Wang Y, Suna A, Mahler W, Kasowski R (1987) J Chem Phys 87:7315
16. Guzelian AA, Banin U, Kadavanich AV, Peng X, Alivisatos AP (1996) Appl Phys Lett 69:1432
17. Schlamp MC, Peng X, Alivisatos AP (1997) J Appl Phys 82:5837
18. Sze SM (1981) Physics of semiconductor devices. Wiley, New York